Bull. Mater. Sci., Vol. 27, No. 6, December 2004, pp. 547–553. © Indian Academy of Sciences.

Impedance analysis of $Pb_2Sb_3LaTi_5O_{18}$ ceramic

C K SUMAN, K PRASAD* and R N P CHOUDHARY†

University Department of Physics, T.M. Bhagalpur University, Bhagalpur 812 007, India
†Department of Physics & Meteorology, Indian Institute of Technology, Kharagpur 721 302, India

MS received 18 June 2004; revised 4 October 2004

Abstract. Polycrystalline sample of $Pb_2Sb_3LaTi_5O_{18}$, a member of tungsten–bronze (TB) family, was prepared using a high temperature solid-state reaction technique. XRD analysis indicated the formation of a single-phase orthorhombic structure. The dielectric studies revealed the diffuse phase transition and the transition temperature was found to be at 52°C. Impedance plots were used as tools to analyse the sample behaviour as a function of frequency. Cole–Cole plots showed Debye relaxation. The activation energy was estimated to be 0·634 eV from the temperature variation of d.c. conductivity. The nature of variation of d.c. conductivity with temperature suggested NTCR behaviour.

Keywords. $Pb_2Sb_3LaTi_5O_{18}$; impedance; phase transition; dielectric constant; orthorhombic structure.

1. Introduction

Among a large number of ferroelectric oxides of different structural families (e.g. perovskite, tungsten-bronze, layered, etc) available now-a-days, some rare-earth doped compounds of tungsten-bronze (TB) family such as (Sr, Ba) Nb_2O_6 (Glass 1981; Ho *et al* 1981; Nagata *et al* 1981; Elissalde and Ravez 1998; Póva *et al* 1998; Kakimoto *et al* 2001), (Pb, Ba)Nb_2O_6 (Francombe 1960; Póva *et al* 1998), $Pb_2Bi_4Ti_5O_{18}$ (Lines and Glass 1977), (Pb, K)$LiTa_{10}O_{30}$ (Hornebecq *et al* 2003), $Ba_2NaNb_5O_{15}$ (Keitsiro 1976), $Ba_2Na_3RNb_{10}O_{30}$ (R = rare-earth ions) (Singh *et al* 1992), $Ba_5RTi_3Nb_7O_{30}$ (R = Dy, Sm) (Shannigrahi *et al* 1998), (R = Nd, Eu, Gd) (Choudhary *et al* 1999), $Ba_4R_2Ti_4Nb_6O_{30}$ (R = Y, Sm, Dy) (Palai *et al* 2001), $Ba_5Nd(Ti, Zr)Nb_7O_{30}$ (Panigrahi *et al* 2002), $Ba_{6-x}La_xNb_{10}O_{30+d}$ (Hwang and Kwon 1997), $Pb_2Bi_3NdTi_5O_{18}$ (Suman *et al* 2003), $(Ba_{1-x}Sr_x)_2NaNb_5O_{15}$ (Rao *et al* 2003), etc have been found attractive because of their promising physical properties suitable for the fabrication of various electronic devices for industrial applications. The crystal structure of this family is based on the framework of corner sharing of distorted BO_6 octahedra in such a way that three different types of interstitial sites (A, B, C) are available for cation substitutions (Jamieson *et al* 1965; Rawan 1998). It has been found that a large number of substitution at these sites can be made to enhance their physical properties needed for the devices such as electro-optic modulator, nonlinear optical devices, pyroelectric sensors, acousto-optic devices, etc (Toledano 1975; Megumi *et al* 1976; Neurgaonkar *et al* 1981; Neurgaonkar and Cory 1986; Hornebecq *et al* 2003; Ohsato and Imaeda 2003; Rao *et al* 2003).

Continuous attempts have been made to investigate $Pb_2A_3RTi_5O_{18}$ (A ≡ Sb or Bi; R ≡ rare-earth ions) compounds with desired characteristics from both theoretical and application points of view. Recent studies on the electrical properties of $Pb_2Bi_3NdTi_5O_{18}$, $Pb_2Bi_3GdTi_5O_{18}$ and $Pb_2Sb_3DyTi_5O_{18}$ ceramic showed the presence of diffuse phase transition (Suman *et al* 2003, 2004a,b). Also, ceramic $Pb_2Bi_3DyTi_5O_{18}$ showed reasonably high value of pyroelectric coefficient and figure of merit (Suman *et al* 2004c). Attractive pyroelectric properties make these compounds suitable for pyroelectric infrared (IR) detector or sensing devices. Keeping in view the importance of the material and non-availability of electrical data, the structural and electrical properties of $Pb_2Sb_3LaTi_5O_{18}$ (abbreviated as PSLT) ceramic are reported. A.c. impedance methods are widely used to characterize ferroelectric materials as the electrical properties of such materials largely depend on grain, grain boundary and/or interface/polarization contributions. In order to understand them, all these contributions must separately be investigated. Accordingly, the results of PSLT have been analysed through impedance spectroscopic technique.

2. Experimental

A mixed high temperature solid-state reaction oxide method was used for the preparation of $Pb_2Sb_3LaTi_5O_{18}$ (PSLT) ceramic:

$$2PbO + \frac{3}{2}Sb_2O_3 + \frac{1}{2}La_2O_3 + 5TiO_2 \xrightarrow{\Delta} Pb_2Sb_3LaTi_5O_{18}.$$

The initial AR-grade powders of PbO, Sb_2O_3, La_2O_3 and TiO_2 were ground and heated at 1050°C for 10 h in air atmosphere. Two percent extra PbO was added to compensate lead loss. The calcined powder was then ground and

*Author for correspondence

put in form of disks (9 mm diameter). The optimized sintering conditions were 1090°C for 6 h in a closed medium. Completion of the reaction and the formation of the desired compound were checked by X-ray diffraction technique. The XRD spectra were taken on calcined powders of PSLT at room temperature using CuK_a radiation (l = 0·15418 nm) over a wide range of Bragg angles ($20° \leq 2q \leq 80°$) with a scanning speed of 2° min^{-1}. A sintered pellet was polished and electroded with air-drying silver paste to measure the electrical properties. Electrical impedance (Z), phase angle (q), loss tangent and capacitance (C) were measured as a function of frequency (0·1 kHz–1 MHz) at different temperatures (20–500°C) using a computer controlled LCR Hi-Tester (HIOKI 3532-50), Japan. Temperature dependence of d.c. conductivity was measured using Keithley-617 electrometer.

3. Results and discussion

3.1 *XRD analysis*

Figure 1 shows the XRD pattern of PSLT at room temperature. A standard computer program (POWD) has been utilized for the XRD-profile fitting. Good agreement between the observed (d_{obs}) and calculated (d_{cal}) inter-planar spacing (table 1) and no trace of any extra peaks due to constituent oxides were found, suggesting that the compound is having a single-phase orthorhombic structure. The lattice parameters were found to be: a = 9·035(0) Å, b = 6·690(2) Å and c = 9·801(5) Å with an estimated error of $\pm 10^{-3}$ Å. The criterion adopted for evaluating the rightness, reliability of the indexing and the structure of PSLT was the sum of differences in observed and calculated d-values [i.e. $\Sigma\Delta d = \Sigma(d_{obs}–d_{calc})$], which were found to be minimum. The unit cell volume ($a \times b \times c$) was calculated to be 592·46 $Å^3$.

3.2 *Impedance analysis*

Figure 2 shows the variation of the real part of impedance (Z') with frequency at several temperatures. It is observed that the magnitude of Z' decreases with the increase in both frequency as well as temperature. The Z' values for all temperatures merge above 100 kHz. This may be due to the release of space charges. The curves also display single relaxation process and indicate an increase in a.c. conductivity with temperature and frequency.

Figure 3 shows the variation of the imaginary part of impedance (Z'') with frequency at different temperatures. The curves show that the Z'' values reach a maxima peak (Z''_{max}) for the temperatures ≥ 400°C. This also indicates the single relaxation process in the system. For the temperature below 400°C, the peak was beyond the range of frequency measurement. The value of Z''_{max} shifts to higher frequencies with increasing temperature. The relaxation times (t) were calculated from the frequency at which Z''_{max} is observed. The frequency for the maximum f_p, called relaxation frequency, shifts to higher values with increasing temperature indicating the increasing loss in the sample. The peak heights are proportional to bulk resistance (R_b) according to equation

$$Z'' = R_b[wt/(1 + w^2t^2)],$$

in Z'' vs frequency plots (Von Hipple 1954). Inset of figure 3 shows the normalized imaginary parts, Z''/Z''_{max}, of the impedance as a function of frequency for PSLT at several temperatures. It seems that high temperature triggers another relaxation process. The Z''/Z''_{max} parameter exhibits a peak with a slightly asymmetric degree at each

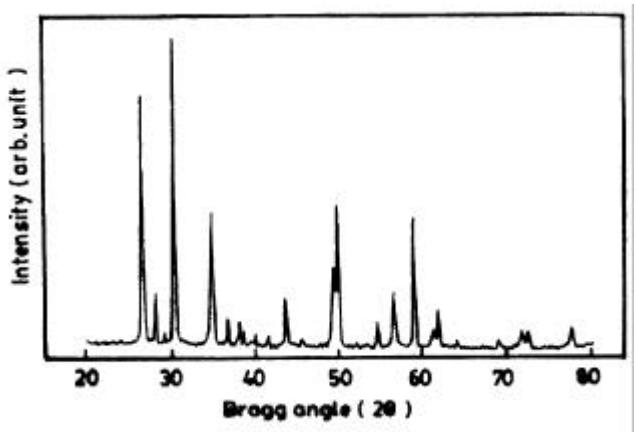

Figure 1. XRD pattern of $Pb_2Sb_3LaTi_5O_{18}$ at room temperature.

Table 1. Comparison of observed and calculated d-values (Å) of some reflections for $Pb_2Sb_3LaTi_5O_{18}$ at room temperature.

$h\ k\ l$	d_{obs} (Å)	d_{cal} (Å)
2 0 2	3·3180	3·3216
0 2 1	3·1644	3·1658
1 0 3	3·0717	3·0725
0 1 3	2·9402	2·9358
3 0 2	2·5643	2·5659
2 1 3	2·4630	2·4616
0 0 4	2·4487	2·4504
2 2 2	2·3547	2·3570
4 0 0	2·2594	2·2587
0 3 1	2·1744	2·1745
3 1 3	2·1020	2·1022
0 2 4	1·9774	1·9768
3 2 3	1·8476	1·8465
3 1 4	1·8275	1·8284
3 3 2	1·6834	1·6832
0 0 6	1·6332	1·6336
4 3 1	1·5655	1·5665
5 2 2	1·5122	1·5123
6 0 0	1·5060	1·5058
3 3 4	1·4469	1·4466
6 2 1	1·3602	1·3598
0 3 6	1·3179	1·3178
1 3 6	1·3043	1·3040
4 3 5	1·2334	1·2334

temperature especially at higher temperatures. At the peak, the relaxation is defined by the condition

$$w_m\ t_m = 1, \quad (1)$$

where t_m is the relaxation time. Figure 4 shows that the relaxation frequency obey the Arrhenius relation given by

$$w_m = w_0 \exp(-E_t/k_B T), \quad (2)$$

where w_0 is the pre-exponential factor. The activation energy, E_t, calculated from least squares fit to log w_m –1/T data is 0·786 eV.

Figure 5 shows the variation of Z' as a function of temperature at various frequencies. All curves present two peaks. The first maxima occur at 52°C at all frequencies, which also resembles with dielectric data (figure 11). The second one occurs at 325°C at 1 kHz and shifts to higher temperature side as frequency increases. This also indicates the relaxation process in the sample, which increases with temperature.

Figure 6 shows a set of impedance data taken over a wide frequency range (100 Hz–1 MHz) at several temperatures as a Nyquist diagram. The impedance data at room temperature do not take the shape of a semicircle in the Nyquist plot rather presents a straight line with large slope, suggesting the insulating behaviour of PSLT at room temperature (inset of figure 6). It is observed that with the increase in temperature the slope of the lines decreases and they curve towards real (Z′) axis and at temperature above 250°C, a semicircle could be traced, indicating increase in conductivity of the sample. All these curves start at almost same value and do not coincide with origin and hence there is a series resistance, 623 Ω, that can be ascribed to the LCR circuit representation of the sample. At higher temperatures (375°C onwards) two semicircles could be obtained with different values of resistance for grain and grain boundary. Hence grain and grain boundary effects could be separated at these temperatures. These compounds are expected to loose traces of oxygen during sintering at high temperature as per the reaction (Kröger and Vink 1956)

$$O_0 \rightarrow \tfrac{1}{2} O_2 \uparrow + V_0^{\bullet\bullet} + 2e^-.$$

These defects affect impedance and capacitance in the formation of barrier layers at the grain–grain boundary interface (Da and Yan 1982). During cooling of the samples

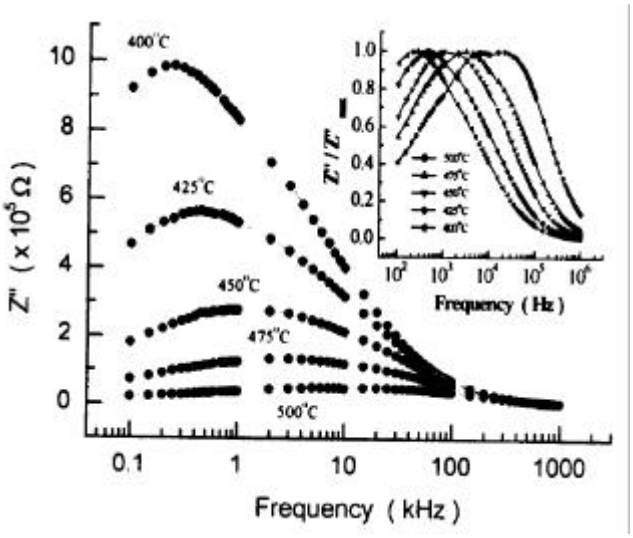

Figure 3. Variation of imaginary part of impedance of $Pb_2Sb_3LaTi_5O_{18}$ with frequency at different temperatures. (Inset: Normalized imaginary parts, Z''/Z''_{max}, of the impedance as a function of frequency for $Pb_2Sb_3LaTi_5O_{18}$ at several temperatures).

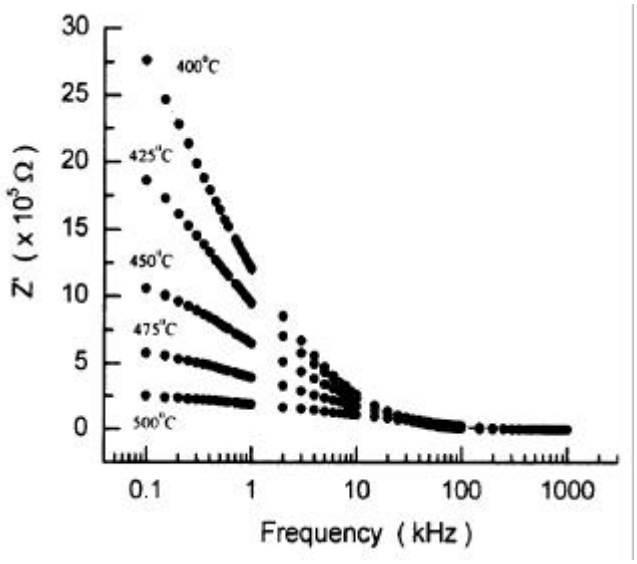

Figure 2. Variation of real part of impedance of $Pb_2Sb_3LaTi_5O_{18}$ with frequency at different temperatures.

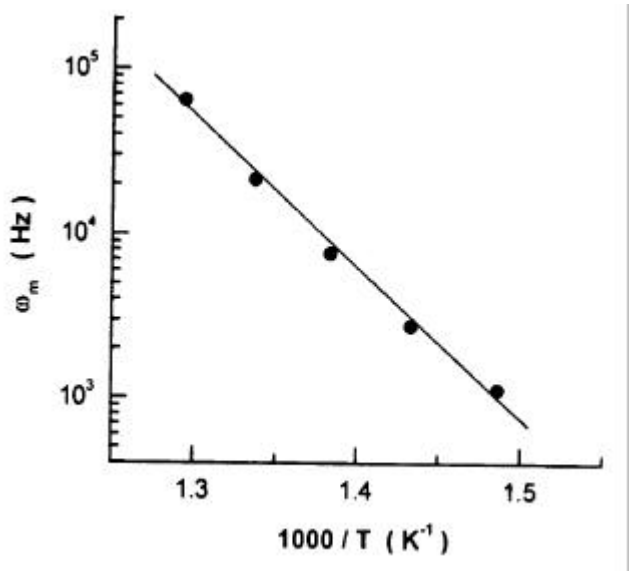

Figure 4. Temperature dependence of relaxation frequency for $Pb_2Sb_3LaTi_5O_{18}$. The circles are the experimental points and the solid line is the least squares straight line fit.

after sintering reoxidation takes place. This oxidation is limited to surface and grain boundaries only due to insufficient time. This results in difference between resistance of grain boundary and grain, giving rise to barrier (Da and Yan 1982). A third semicircle could also be seen at and above 450°C, which could be due to electrode effect. It can also be observed that the peak maxima of the plots decrease with increasing temperature and the frequency for the maximum shifts to higher values with the increase in temperature.

Complex impedance formalism helps in determining inter-particle interaction like grain, grain boundary effects, etc. To study the contribution due to different effects, Cole–Cole analyses have been done at different temperatures. It also provides information about the nature of dielectric relaxation. For pure monodispersive Debye process, one expects semicircular plots with the centre located on the Z'-axis whereas, for polydispersive relaxation, these argand plane plots are close to circular arcs with endpoints on the axis of reals and the centre below this axis. The complex impedance in such situations is known to be described by Cole–Cole formalism (Cole and Cole 1941)

$$Z^*(w) = Z' + iZ'' = R/[1 + (iw/w_0)^{1-a}], \quad (3)$$

where a represents the magnitude of the departure of the electrical response from an ideal condition and this can be determined from the location of the centre of the Cole–Cole circles. When a goes to zero ($1 - a \rightarrow 1$), (3) gives rise to classical Debye's formalism. Figure 7 depicts two representative plots for $T = 425$ and 500°C. It can be seen from these plots that the data is represented by full semicircle i.e. semicircle centred on the abscissa axis ($a = 0$), suggests that the relaxation to be of Debye type. The resistance of bulk (R_b), grain boundary (R_{gb}) and interface/polarization (R_e), could directly be obtained from the intercept on the Z'-axis. The capacitances (C_b, C_{gb} and C_e) due to these effects can be calculated using the relation

$$w R C = 1, \quad (4)$$

where w is the angular frequency at the maxima of the semicircle for the component. Figure 8 shows the temperature variation of R_b, R_{gb}, R_e, C_b, C_{gb} and C_e obtained from Cole–Cole plots at different temperatures. It can be seen that the values of R_b, R_{gb}, R_e, C_b and C_{gb} decrease while the value of C_e increases with the increment in temperature. The increase of C_e with temperature may be due to the fact that the electrode polarization increases with temperature. From the peak of each semicircle of Cole–Cole plots

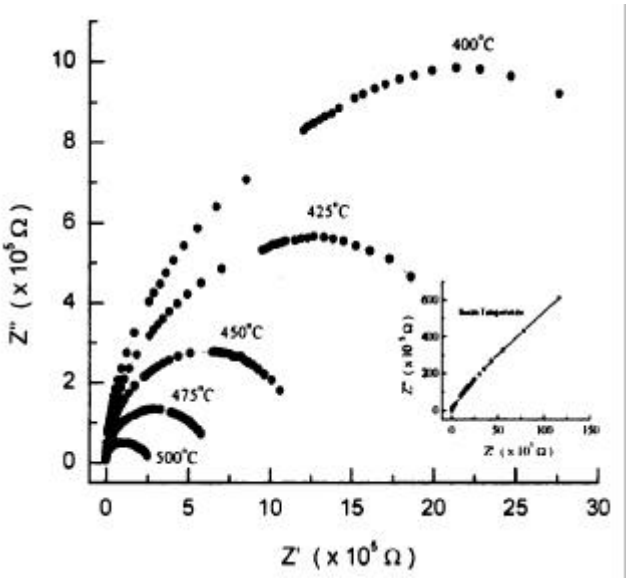

Figure 6. Nyquist diagram for $Pb_2Sb_3LaTi_5O_{18}$ at different temperatures. (Inset: Nyquist diagram for $Pb_2Sb_3LaTi_5O_{18}$ at room temperature).

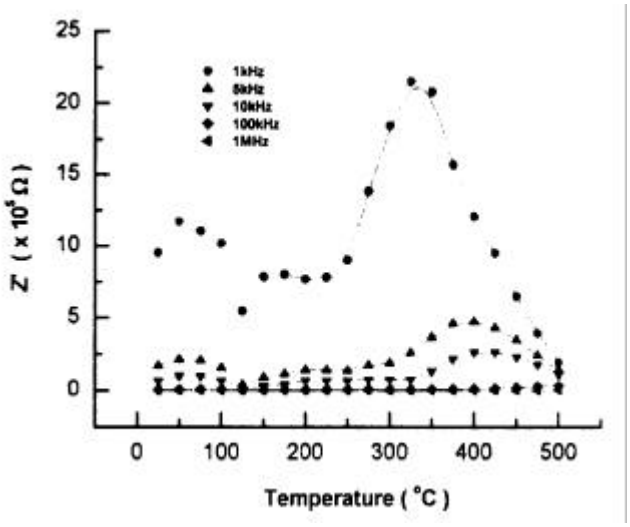

Figure 5. Variation of real part of impedance of $Pb_2Sb_3LaTi_5O_{18}$ with temperature at different frequencies.

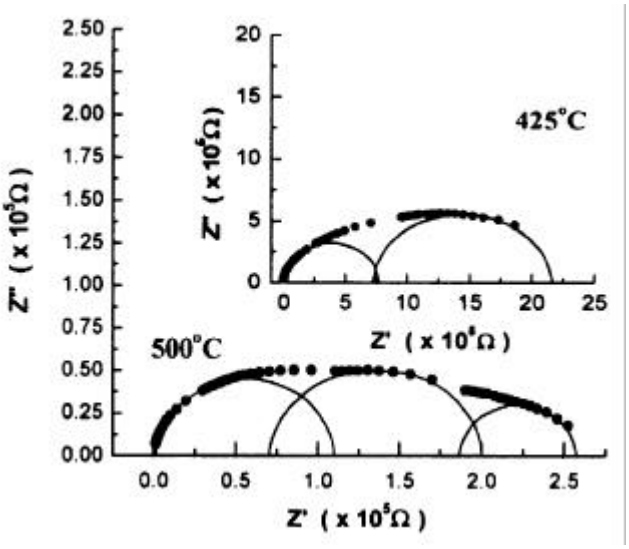

Figure 7. Cole–Cole plots at temperatures of 425°C and 500°C for $Pb_2Sb_3LaTi_5O_{18}$.

the relaxation times due to different effects were estimated. Figure 9 shows the variation of relaxation times t_b, t_{gb} and t_e with inverse of temperature. These plots are almost linear and obeys an Arrhenius relationship

$$t = t_0 \exp(E_a/k_B T), \quad (5)$$

where E_a is the activation energy for conduction. The values of activation energy due to different contributions as obtained by least squares fitting are E_b = 0·304 eV, E_{gb} = 0·528 eV and E_e = 0·165 eV.

The Bode plot (figure 10) at room temperature suggests the capacitive behaviour of electrode as log|*Z*| varies linearly with log*f* with a slope of – 0·9639, which is very close to the theoretical value of – 1 for a pure capacitor. Also the value of *q* decreases with the increase in frequency and it lies in the range of – 90° to – 80°. Under these conditions, |*Z*| is related with frequency as

$$\log|Z| = -\log f - \log C_{bl},$$

where C_{bl} represents the barrier layer capacitance. When f = 1, $\log|Z| = -\log C_{bl}$. The value of C_{bl} obtained from figure 10 is 16·76 nF. This value is comparable with $Pb_2Sb_3DyTi_5O_{18}$ (Suman *et al* 2004b). The value of log|*Z*| and *q* at 1 kHz were found respectively to be 6·8902 and – 82·99° at room temperature.

3.3 *Dielectric analysis*

Figure 10 shows the variation of *e* and tan*d* with frequency at room temperature. The values of both *e* as well as tan*d* were found to decrease with the increase in frequency. This typical behaviour indicates that PSLT behaves like normal ferroelectric material where different types of polarization mechanisms might be present. We find a similar dielectric behaviour with respect to frequency in other compounds of this family (Suman *et al* 2003, 2004a–c).

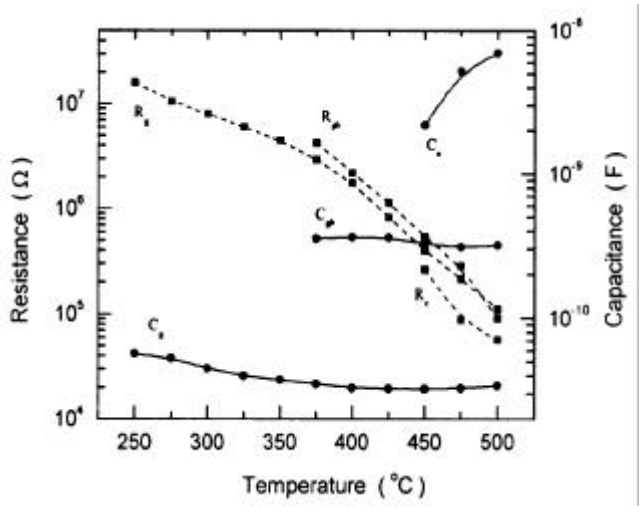

Figure 8. Variation of resistance and capacitance for grain, grain boundary and electrode contributions with temperature of $Pb_2Sb_3LaTi_5O_{18}$.

The room temperature value of *e* and tan*d* at 1 kHz were found to be 119 and 0·12, respectively.

To understand the dielectric anomalies, temperature variation of dielectric measurements were carried out on PSLT and are presented in figure 11. Both *e*–*T* as well as tan *d*–*T* plots show a broad maximum at ferro-paraelectric phase transition temperature (T_C). It has been observed that maxi-

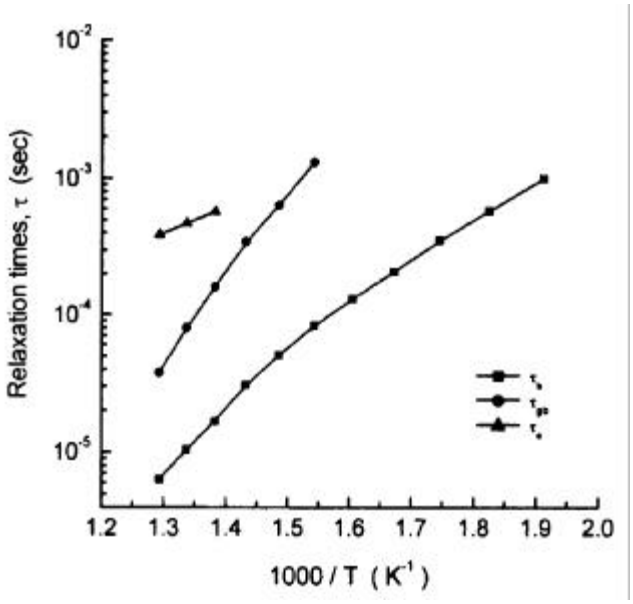

Figure 9. Variation of relaxation time for grain, grain boundary and electrode contributions with inverse of temperature for $Pb_2Sb_3LaTi_5O_{18}$.

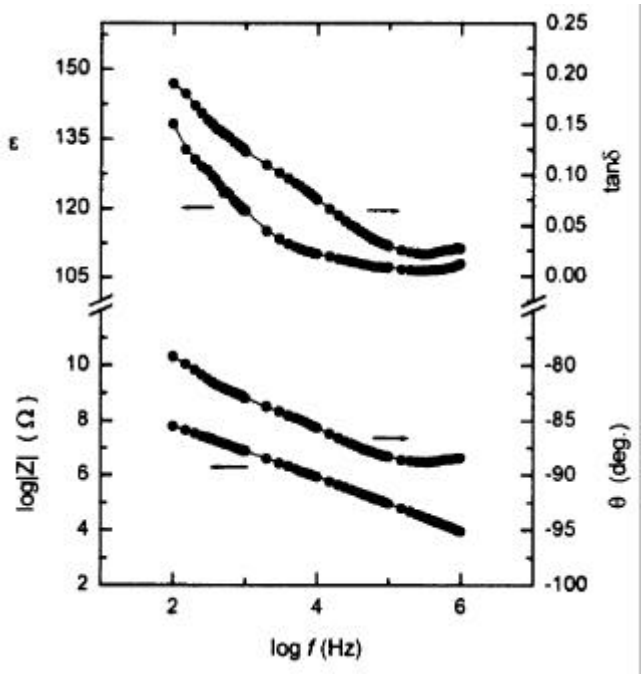

Figure 10. Variation of *e*, tan *d*, log |*Z*| and *q* of $Pb_2Sb_3LaTi_5O_{18}$ with frequency at room temperature.

mum value of e (e_{max}) decreases (from 155 at 10 kHz to 101 at 1 MHz) and e–T curve flattens with the increase in frequency. The dielectric data beyond 52°C, in the paraelectric region did not fit to Curie–Weiss law. A convenient way of studying deviation from Curie–Weiss law, is to fit into diffuse phase transition (DPT) type, using the relation (Uchino and Nomura 1982)

$$1/e - 1/e_{max} = A(T - T_C)^g, \quad (6)$$

where A is a constant and g is called the diffusivity parameter giving the measure of broadness in phase transition and normally varies between 1 and 2. To estimate the diffusivity parameter, g, the experimental data at $T > T_C$, were fitted to (6) by the method of least squares. The value of g so obtained is 1·22, which clearly indicates the DPT. The occurrence of diffuse phase transition (DPT) may be due to substitutional randomness or inhomogeneity in atomic sites and size of the substituted ions where the local curie points of different microregions are statistically distributed around the mean curie temperature (Prasad 2000).

3.4 *Conductivity analysis*

Figure 12 shows the electrical conductivity, $s(w)$, of PSLT as a function of frequency at different temperatures in the paraelectric phase. The conductivity depends on frequency according to the 'universal dynamic response' for ionic conductors (Grigas 1996) given by the phenomenological law

$$s(w) = s_{d.c.} + A \cdot w^n,$$

where A is a thermally activated quantity and n the frequency exponent and can take the value < 1. It is observed that variation of $s(w)$ with frequency shows flattening with increment in temperature (≥ 450°C). The switch from the frequency-independent $s_{d.c.}$ to the dependent $s(w)$ regions shows the onset of the conductivity relaxation phenomenon and the translation from long range hopping to the short range ion motion (Mizaras *et al* 1997). The dispersion in conductivity at low frequencies may be due to the electrode polarization. The inset of figure 12 shows the variation of d.c. conductivity (ln $s_{d.c.}$) against $10^3/T$. The nature of variation is almost linear over a wide temperature region indicating the ohmic nature of contact and conductivity obeys the Arrhenius relationship

$$s_{d.c.} = s_0 \exp(-E_a/k_B T),$$

where E_a is the activation energy of conduction and T the absolute temperature. The nature of variation shows the negative temperature coefficient of resistance (NTCR) behaviour of PSLT. The value $E_a = 0{\cdot}634$ eV was obtained by least squares fitting of the data at higher temperature region. The low value of activation energy obtained could be attributed to the influence of electronic contribution to the conductivity. This value is comparable to other TB-type ferroelectric oxides (Suman *et al* 2003, 2004a–c). The value of R^2 (regression coefficient indicating goodness of fit) for all the fittings, quoted in this paper, is in excess of 0·995.

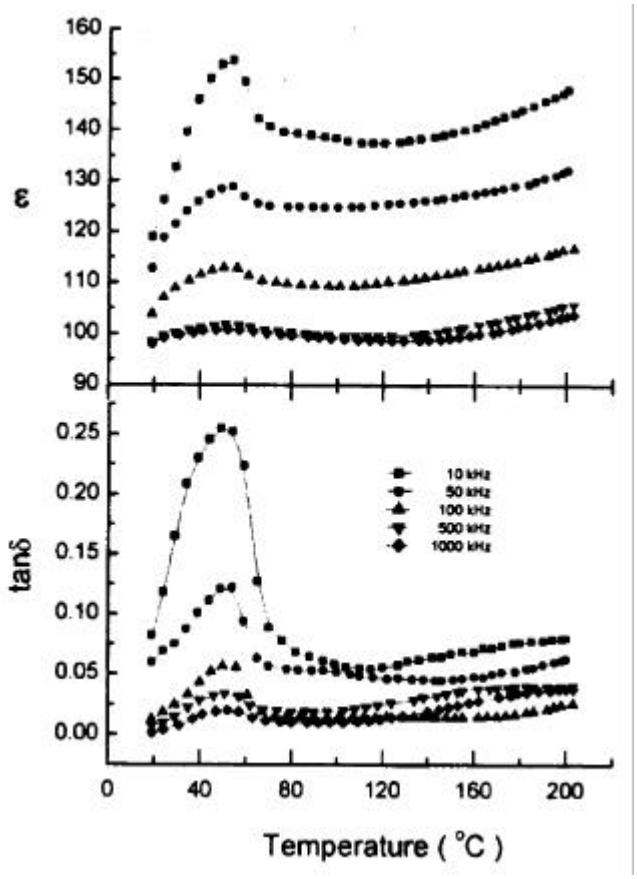

Figure 11. Variation of dielectric constant and loss tangent of $Pb_2Sb_3LaTi_5O_{18}$ with temperature at different frequencies.

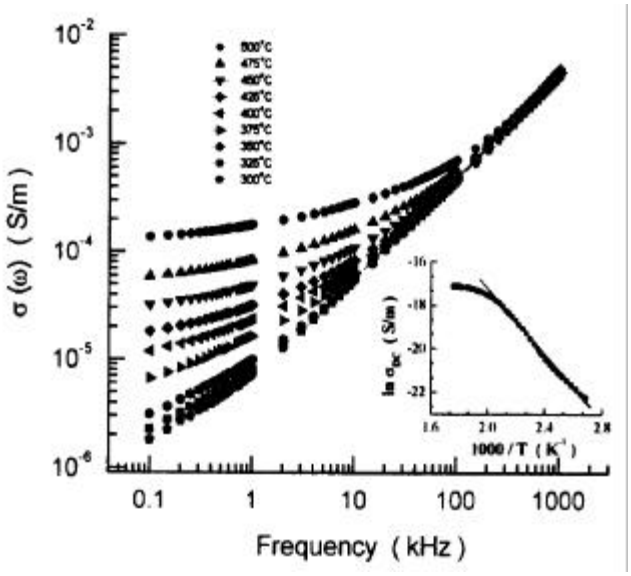

Figure 12. Variation of a.c. conductivity of $Pb_2Sb_3LaTi_5O_{18}$ with frequency at different temperatures. (Inset: Temperature dependence of d.c. conductivity of $Pb_2Sb_3LaTi_5O_{18}$).

4. Conclusions

It is concluded that PSLT has orthorhombic structure at room temperature and undergoes diffuse phase transition at 52°C. Also, PSLT has low dielectric constant, low loss and low conductivity. Impedance analyses indicated the capacitive behaviour of electrode. Sample showed relaxation effects and indicated that the relaxations are of Debye type. The relaxational frequencies shifted to higher frequencies with the increase of temperature. The nature of variation of d.c. conductivity with temperature suggested NTCR behaviour with activation energy, 0·634 eV.

References

Choudhary R N P, Shannigrahi S R and Singh A K 1999 *Bull. Mater. Sci.* **6** 975

Cole K S and Cole R H 1941 *J. Chem. Phys.* **9** 341

Da Ren Chen and Yan Y G 1982 *Electronic Elements Materials* **1** 25

Elissalde C and Ravez J 1998 *J. Kor. Phys. Soc.* **32** S1022

Francombe M H 1960 *Acta Crystallogr.* **13** 131

Glass A M 1981 *J. Appl. Phys.* **40** 4699

Grigas J 1996 *Microwave dielectric spectroscopy of ferroelectrics and related materials* (Amsterdam: Gordon and Breach Publn. Inc.)

Ho W W, Hall W F, Neurgaonkar R R, Dewames R E and Mim T L 1981 *Ferroelectrics* **38** 833

Hornebecq V, Elissalde C, Porokhonskyy V, Bovtun V, Petzelt J, Gregara I, Maglione M and Ravez J 2003 *J. Phys. Chem. Solids* **64** 471

Hwang Y K and Kwon Y U 1997 *Mater. Res. Bull.* **32** 1495

Jamieson P B, Abraham S C and Bernstein J L 1965 *J. Chem. Phys.* **48** 5048

Kakimoto K, Kakemoto H, Baba A, Fujita S and Masuda Y 2001 *J. Euro. Ceram. Soc.* **21** 1569

Keitsiro A 1976 *J. Phys. Soc. Jpn.* **41** 880

Kröger F A and Vink H J 1956 *Solid State Phys.* **3** 307

Lines M E and Glass A M 1977 *Principle and applications of ferroelectric and related materials* (Oxford: Clarendon Press)

Megumi K, Nagatsuma N, Kashiwada Y and Furuhata Y 1976 *J. Mater. Sci.* **11** 1583

Mizaras R, Takashige M, Banys J, Kojima S, Grigas J, Hamazaki Sin-Ichi and Brilingas A 1997 *J. Phys. Soc. Japan* **66** 2881

Nagata K, Yamamoto Y, Igarashi H and Okazaki K 1981 *Ferroelectrics* **38** 853

Neurgaonkar R R and Cory W K 1986 *J. Opt. Soc. Am.* **3** 274

Neurgaonkar R R, Cory W K, Ho W W and Hall W F 1981 *Ferroelectrics* **38** 857

Ohsato H and Imaeda M 2003 *Mater. Chem. Phys.* (in print)

Palai R, Choudhary R N P and Tewari H S 2001 *J. Phys. Chem. Solids* **62** 695

Panigrahi A, Singh N K and Choudhary R N P 2002 *J. Phys. Chem. Solids* **63** 213

Póva J M, Moreira E N, Garcia D, Spínola D U P, do Carmo C G V and Eiras J A 1998 *J. Kor. Phys. Soc.* **32** S1046

Prasad K 2000 *Ind. J. Engg. Mater. Sci.* **7** 446

Rao K S, Prasad T N V K V, Subrahmanyam A S V, Lee J H, Kim J J and Cho S H 2003 *Mater. Sci. Engg.* **B98** 279

Rawan C J 1998 *J. Mater. Res.* **13** 187

Shannigrahi S R, Choudhary R N P, Kumar A and Acharya H N 1998 *J. Phys. Chem. Solids* **59** 737

Singh K S, Sati R and Choudhary R N P 1992 *J. Mater. Sci. Lett.* **11** 788

Suman C K, Prasad K and Choudhary R N P 2003 *Mater. Chem. Phys.* **82** 140

Suman C K, Prasad K and Choudhary R N P 2004a *Indian J. Phys.* **78** 855

Suman C K, Prasad K, Choudhary S N and Choudhary R N P 2004b *Indian J. Phys.* **78** 849

Suman C K, Prasad K and Choudhary R N P 2004c *Phys. Status Solidi (a)* **201** 3166

Toledano J C 1975 *Phys. Rev.* **B12** 943

Uchino K and Nomura S 1982 *Ferroelectr. Lett.* **44** 55

Von Hipple R 1954 *Dielectrics and waves* (NY: John Wiley and Sons)